

Prospects for the creation of compact refrigerating machines based on low-speed reciprocating machines

Kobylsky R.E*, Busarov S.S., Kapelyukhovskaya A.A., Busarov I.S.

Omsk State Technical University, Omsk, Russia, 644050, Omsk,

Prospect Mirastr., 11

*corresponding author.

E-mail address: R.E. Kobylsky

Annotation

Currently, refrigerating machines with two-stage compression are most often used to obtain temperatures below minus 40°C. Such compressor designs are cumbersome and technologically complex. At the moment, there is an alternative to multistage compression – the use of low-speed compressors capable of compressing gas to high pressures in one stage at acceptable discharge temperatures. The use of a scheme with a single-stage low-speed compressor makes it possible to increase the refrigeration coefficient by 12 ÷ 20%. At the same time, there is no need to install a heat exchanger-capacitor, which reduces the weight and dimensions of the entire installation on 20%. As can be seen from the results obtained, it is possible to obtain the liquid phase of the refrigerant in the working chamber of the compressor. For low-speed compressors, the presence of liquid is not scary and does not cause hydraulic shocks. However, the study of the condensation process of the working fluid in the compressor requires additional research and must be confirmed experimentally.

Keywords: refrigerating machine, low-speed compressor, working fluid R744, reduction of weight and size parameters, mathematical model, condenser, experimental studies

Date of Submission: 16-08-2024

Date of acceptance: 31-08-2024

I. Introduction

Reciprocating compressors are currently the most applicable types of compressors in small refrigerating machines [1, 2]. In refrigeration technology, it is often necessary to obtain temperatures in the range minus 40 ÷ 60 °C. Such temperatures cannot be obtained in refrigerating machines with a single-stage reciprocating compressor [1-3]. The reason for this is the increased ratio of the condensation pressure to the boiling pressure of the refrigerant (P_c/P_0), which is traditionally limited to a value of 8 for refrigerating machines [4].

The use of reciprocating machines with an increased ratio of discharge pressure to suction pressure in the theory of reciprocating compressors has its own ranges based on generally accepted factors leading to the transition to multistage compression. The most significant of these factors (causes) is an increase in temperature with an increase in pressure. The value of the maximum temperature is limited by safety requirements, ensuring that there is no oil ignition and deformation of the working chamber parts. The second most important is the decrease in productivity associated with the presence of harmful space in the reciprocating compressor. The third factor is the increase in piston forces, which leads to an over-dimensionality of the movement mechanism. The fourth factor is the possibility of reducing indicator performance when implementing two-stage compression. And the fifth of the most significant factors is the decrease in indicator efficiency. All these issues are solved by implementing sequential compression in one stage, cooling the compressed gas and compression to the final pressure in the second stage, the diameter of which is smaller than the diameter of the first stage, which leads to equality of piston forces in the first and second draws [5, 6].

The problems that arise when compressing refrigerants at $P_c/P_0 > 8$ can be solved using low-speed long-stroke compressors [7-9]. It should be noted that the design minimizes the effect of dead volume due to the elongated shape of the cylinder and increases the cycle time to several seconds, this allows you to obtain a degree of

pressure increase exceeding 100-120 with acceptable performance indicators of the workflow. Figure 1 shows a model of such a compressor.

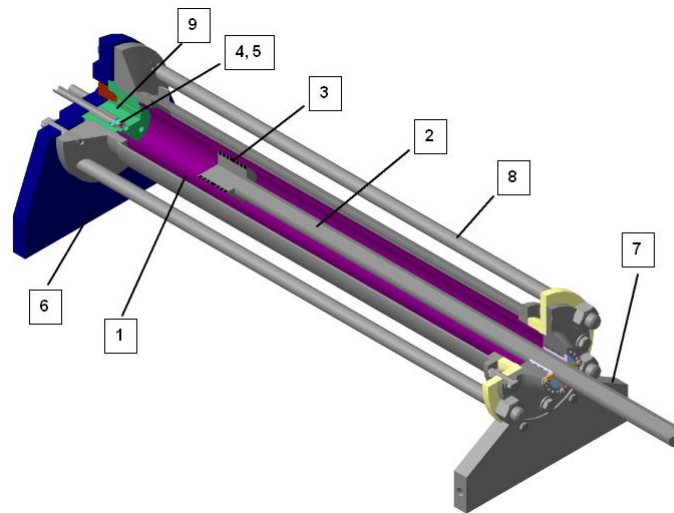


Figure 1 – Low-speed compressor model

To analyze the possible replacement of a refrigerating machine with a two-stage compressor with a machine with a low-speed compressor, we take as a basis the well-known scheme of a two-stage refrigerating machine with double throttling. The use of a low-speed compressor will allow, under the same conditions, to implement a single-stage compression scheme.

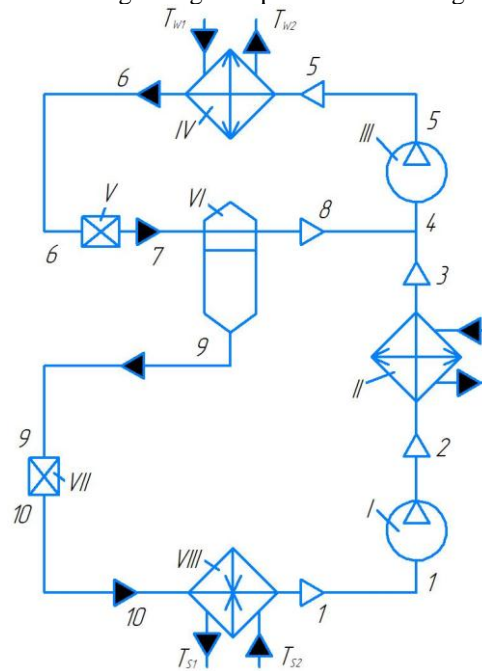


Figure 2 – Diagram of a two-stage refrigeration unit with double throttling:

1-2 Compression in the first stage; 2-3 Intermediate cooling; 3-4 Compression in the second stage; 4-5 Condensation; 5-6 Throttling; 6-7 Throttling; 7-8 Throttling; 8-9 Throttling; 9-10 Throttling; 10-1 Evaporation

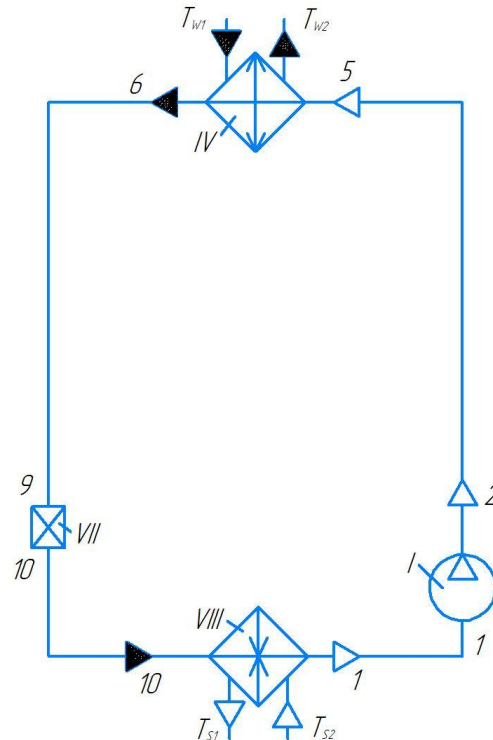


Figure3–Diagram of a refrigeration unit with a low-speed compressor: 1-2 Compression; 5-6 Condensation; 9-10 Throttling; 10-1 Evaporation

A preliminary analysis of the installations shown in Figures 2.3 suggests a significant simplification of the circuit using a low-speed compressor with the possibility of significantly reducing the capacitor or excluding it from the circuit.

In modern small refrigerating machines, for example, in such low-temperature machines based on COPELAND compressors (Germany), condenser units account for 15-25% of the weight and size parameters of the entire installation (Table 1).

Table1–Characteristics of small refrigerating machines

Model Condenser/Compressors	Cooling capacity (W) $t_{w2} = \text{minus } 70^{\circ}\text{C}$; $t_{w1} = \text{plus } 32^{\circ}\text{C}$	Power consumption H.M. (W)	Refrigerant
MDE114-4/AK-D4SL-150X/D4SL-1500	6050	17160	R22, R23
MDE114-4/AK-D4SL-200X/D4ST-2000	6690	18160	
MDE123-4/AK-D6ST-320X/D4ST-3200	10100	29640	

The presented data indicate the urgency of the problem of reducing the load on the capacitor. Based on the experimental studies presented below, a mathematical model of a low-speed refrigeration compressor will be created.

The object of the study

Carbon dioxide (R744) is widely used in the food industry for freezing products [13], is environmentally safe and has a low critical temperature, is compatible with almost all structural materials, but cannot condense at temperatures above plus 31 °C. The low-speed compressor in question is hermetically sealed and grease-free. A working chamber with a diameter of 0,05 m and a piston stroke of 0,5 m, the working process time is 2-4 seconds.

The stage has external water cooling. Initial conditions: suction temperature 293 K; suction pressure 0,5 MPa, the degree of pressure increase is 100. The refrigerant is R744. Based on the experimental studies presented below, a mathematical model of a low-speed refrigeration compressor will be created.

Experimental research methodology

An experimental study of the working processes of the compressor stage under consideration involves measuring its actual performance and indicator power, the average discharge temperature, as well as the

instantaneous parameters of the compressible working fluid. These results will allow us to determine the efficiency of the working process and the heat transfer coefficient on the inner surface of the working chamber.

An experimental stand with a linear (hydraulic) drive has been developed for conducting experimental studies. The general view of the experimental stand from the studied stage of the reciprocating compressor is also represented by a suction cylinder Fig.3. The linear actuator in this scheme is a hydraulic drive. The measuring circuit is shown in Fig.4. The operation of the stand is carried out as follows: the piston 1 is driven through the rod 2 from the rod of the hydraulic cylinder, which in turn is driven from the accumulator station. Since the developed stage is a stage without lubrication, the sealing cuffs 3 mounted on the piston 1 are made of self-lubricating material based on PTFE. Carbon dioxide is supplied from the cylinder 10, the pressure of the supplied gas is regulated by a reducer 9. Data from the temperature sensor and pressure sensor are transmitted to the digital oscilloscope 7 through an amplifier 6. The gas flow rate at the outlet is measured by a flow meter 8, the signal from which is also transmitted to the digital oscilloscope 7 through an amplifier 6. The gas flow rate at the outlet is measured by a flow meter 8, the signal from which is also transmitted to the digital oscilloscope 7 through an amplifier 6.



Figure 4— An experimental stand with a slow-moving long-stroke stage

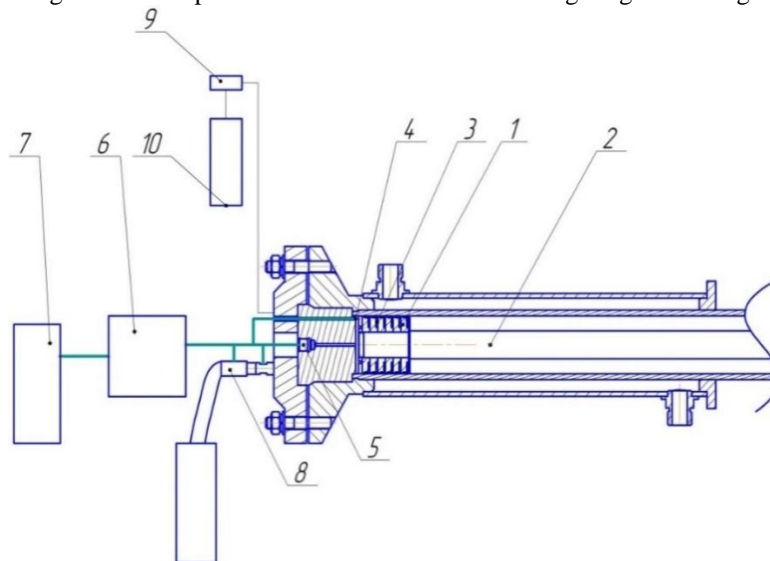


Figure 5— Measuring circuit of the stand

A Honeywell AWM720P1 sensor was used to measure the flow rate. The advantage of this sensor is the digital output signal, which allows it to be connected to modern PCs and oscilloscopes, as well as the factory output characteristic for various gases. The error of this sensor is 2%. Sensors based on a thermistor type ST1-18 A were used to measure the temperature of compressed air [6,7]. The data from the temperature sensor is transmitted to the digital oscilloscope via an amplifier.

Waveforms of instantaneous parameters such as temperature and pressure were obtained. An example of waveforms is shown in Figure 6. The instrument error of pressure measurement is shown below. Let's determine the general error of the temperature sensor based on a bead thermistor [8-10].

$$\delta_T = \sqrt{\delta_{osc}^2 + \delta_t^2 + \delta_v^2 + \delta_F^2}, \tag{1}$$

where δ_{osc} – the relative error of the oscilloscope, 0,05%;

δ_t – the error of the thermometer, determined by the error of the device, 0,1%;

δ_v – the error of the voltmeter, determined by the error of the device, 0,3%;

δ_F – the calculation error according to the interpolated formula obtained, considering the nonlinear dependence of voltage on temperature, 1,5%.

Thus, the error in measuring the instantaneous air temperature in the working chamber of the experimental stage will be:

$$\delta_T = \sqrt{0,05^2 + 0,1^2 + 0,3^2 + 1,5^2} = 1,53 \%$$

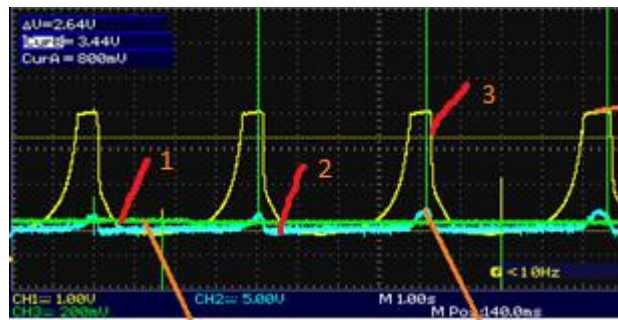


Figure 6 – Parameters of a low-speed compressor at $P_{suc}=0,5\text{MPa}$; $P_{disc}=6,0\text{MPa}$:
1 – flow rate, 2 – temperature, 3 – pressure

Silicon pressure sensors of the D16 type were used to measure gas pressure [11]. The temperature measurement was performed by 4 thermistors with a negative temperature coefficient of resistance. The actual gas flow rate at the injection stage is determined by the AWM720P1 type flow sensor. Data from the temperature sensor, pressure sensor and flow sensor are transmitted to the digital oscilloscope via an amplifier. The instrument error of measuring temperature, pressure and flow is shown below.

Let's determine the instrument error when calibrating the pressure sensor, determined by the formula [9]:

$$\delta_{ps} = \sqrt{\delta_p^2 + \delta_{MPG}^2 + \delta_0^2}, \tag{2}$$

Where δ_p – relative error of the pressure sensor, 1,4 %;

δ_{MPG} – relative error of the model pressure gauge, 1,5 %;

δ_0 – the relative error of the oscilloscope, 3 %.

$$\delta_{ps} = \sqrt{3^2 + 1,5^2 + 1,4^2} = 3,63 \%$$

Determination of integral characteristics

Conducting experimental studies of the working processes of piston units implies the determination of integral characteristics that cannot be determined directly by any device. These parameters include the indicator power of the piston stage, the feed ratio and the isothermal indicator efficiency.

The method of graphical use of the indicator diagram has become the most widespread in determining the indicator power [12]. The experimentally obtained expanded indicator diagram using a pressure sensor is subject to folding to obtain a collapsed diagram representing a closed cycle. The area of the resulting diagram characterizes the experimental indicator work spent, and knowing the cycle time, the indicator power is obtained.

The isothermal indicator efficiency is determined by the ratio of the value of the indicator work obtained according to the experimental graph of the dependence of the instantaneous pressure on the volume of the working chamber to the operation of an ideal isothermal compressor [13]:

$$\eta = \frac{P_{suc} \cdot \bar{V}_h \cdot \ln\left(\frac{P_{disc}}{P_{suc}}\right)}{L_{ind.}} \tag{3}$$

The actual performance of the stage can be measured by the selected flow sensor and recalculated for suction conditions – V_e . Thus, the experimental feed coefficient is defined as the ratio of the actual performance to the performance of an ideal low-speed stage under identical suction conditions, operating and design parameters [13]:

$$\lambda = \frac{V_e}{V_h} \tag{4}$$

The conducted experimental studies made it possible to create a refined methodology for the numerical calculation of a low-speed compressor when operating on carbon dioxide.

Numerical calculation method

The main equation that implements the relationship between the main processes occurring in the working chamber is the equation of the first law of thermodynamics. Let's determine the change in the internal energy of the system [14, 15]:

$$dU = dA \pm dQ \pm (dm \cdot i) \tag{5}$$

where dA – the work performed by the refrigerant or the work performed on the refrigerant, J;
 dQ – the heat withdrawn from the gas or transferred to it from the walls of the working chamber, J;
 $dm \cdot i$ – we characterize the energy entering or removing from the system by gas flows (the product of the mass of the gas and its specific enthalpy), J.

It should be noted that there and further the equations are written for a certain small period of time, where the quantities included in the equations have a constant value for this period of time.

$$dA = P_g \cdot dV, \tag{6}$$

where P_g – the gas pressure, Pa;
 dV – the change in volume (the product of the area of the piston by its speed of movement), m^3 .
 The refrigerant pressure is determined from the equation of state:

$$P_r = \frac{z(P) \cdot m \cdot R \cdot T_g}{V_g}, \tag{7}$$

where m – the current mass of the working fluid in the system, kg;
 $z(P)$ – a function of the change in the compressibility coefficient of the working fluid in question;
 R – the gas constant, J/K;
 V_g – volume of gas, m^3 ;
 T_g – the temperature, there is a function of the energy of the system – U , K.

$$T_r = \frac{U}{m \cdot C_v}, \tag{8}$$

where C_v – the specific mass heat capacity in the isochoric process, J/(kg·K).

$$dQ = \alpha_{avg} \cdot (T_g - T_w) \cdot f, \tag{9}$$

where α_{avg} – the heat transfer coefficient, determined experimentally, $W/m^2 \cdot K$;
 T_w – wall temperature, K;
 f – the heat exchange area, m^2 .
 Heat transfer coefficient [169]:

$$\alpha = \lambda \cdot (\rho/\mu)^x \cdot W^\mu \cdot D^{1-x}_{egu}, \tag{10}$$

where λ, μ, D_{egu} and W – the current values, respectively, of the coefficient of thermal conductivity, dynamic viscosity, equivalent cylinder diameter and conditional gas velocity in the working chamber;
 x – the empirical coefficient,

$$dm = \alpha \cdot \varepsilon \cdot A \cdot \sqrt{2 \cdot \rho \cdot \Delta P}, \tag{11}$$

where α – the consumption coefficient;

A–expiration area, m²;
 ΔP–pressure drop, Pa;
 ρ– the density, kg/m³.

Equation(11) is used to determine mass flows both through valves (open or partially open), then the value of area A includes the variable lifting height of the valve plate (h) and to determine mass flow through leaks. In the case of determining the mass flow through the valve gaps, the values of the conditional gaps obtained experimentally are used. When determining leak through a cylinder piston seal, the area A is the product of the perimeter of the cylinder piston seal by the value of the conditional gap in the cylinder piston seal.

To determine the coordinate of the locking device (h), the following equation is solved:

$$m_{pl} \cdot \ddot{h} = \vec{F}_g + \vec{F}_{sf} + \vec{F}_{ff} + \vec{G} + \vec{F}_{ef}, \tag{12}$$

where \vec{F}_g – the total force acting on the plate from the gas side, N;

\vec{F}_{sf} – the spring's elastic force, N;

\vec{F}_{ff} – the friction force of the gas, N;

\vec{F}_{ef} – the elastic force of an elastomer element;

\vec{G} – the weight of the locking device.

The simplifying assumptions adopted to create this calculation method correspond to those generally accepted for this class of mathematical models [16].

The results of numerical and field experiments were compared. The results of the comparison are shown in Fig. 7-10.

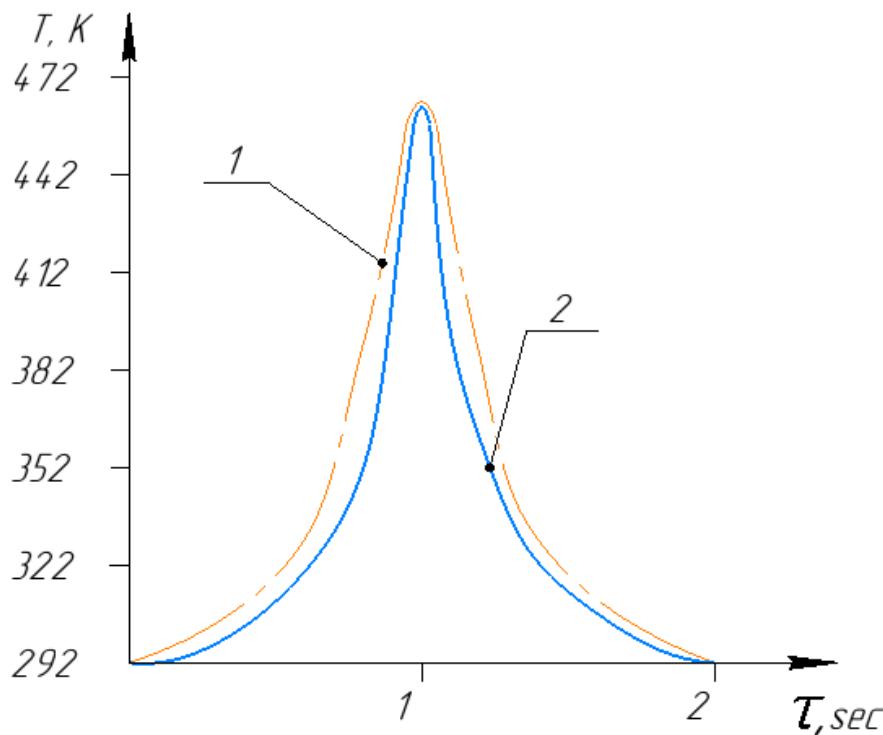


Figure 7–Graph of the instantaneous temperature change during the cycle at a pressure of 10 MPa

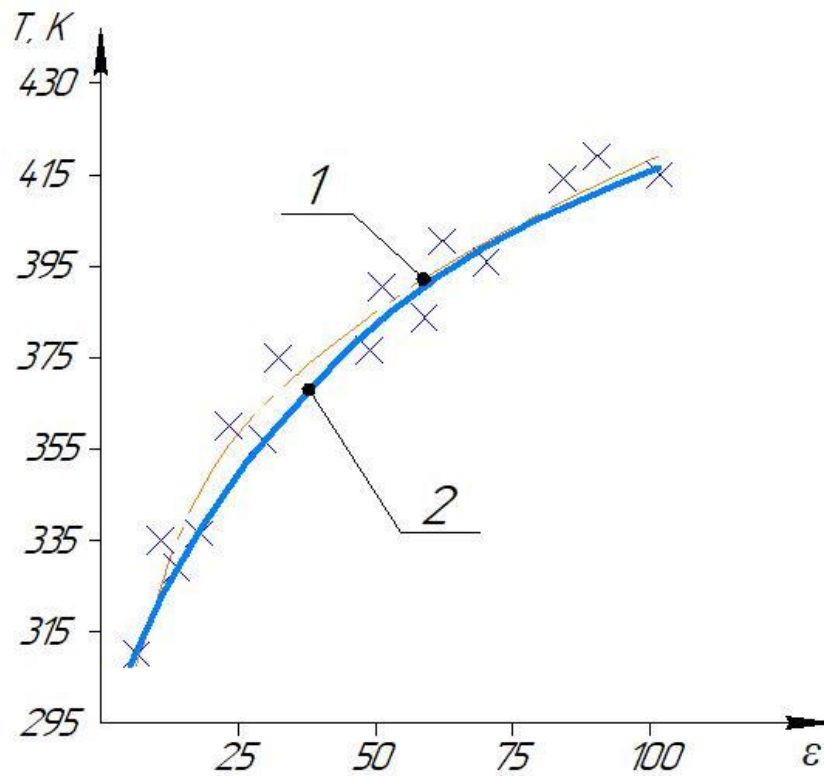


Figure8–Graph of the average temperature changed during the cycle at a pressure of 10MPa

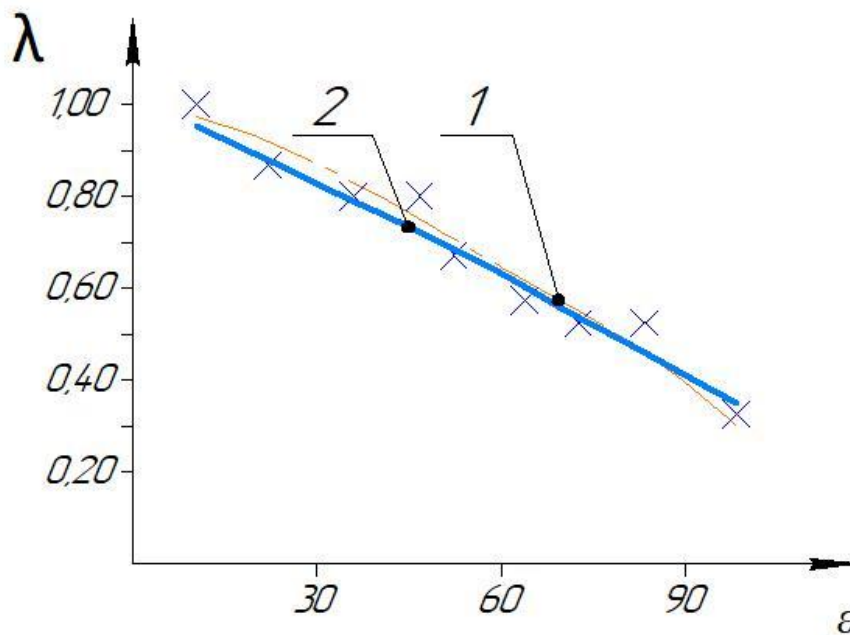


Figure9–Graph of the change in the feed ratio from the degree of pressure increase

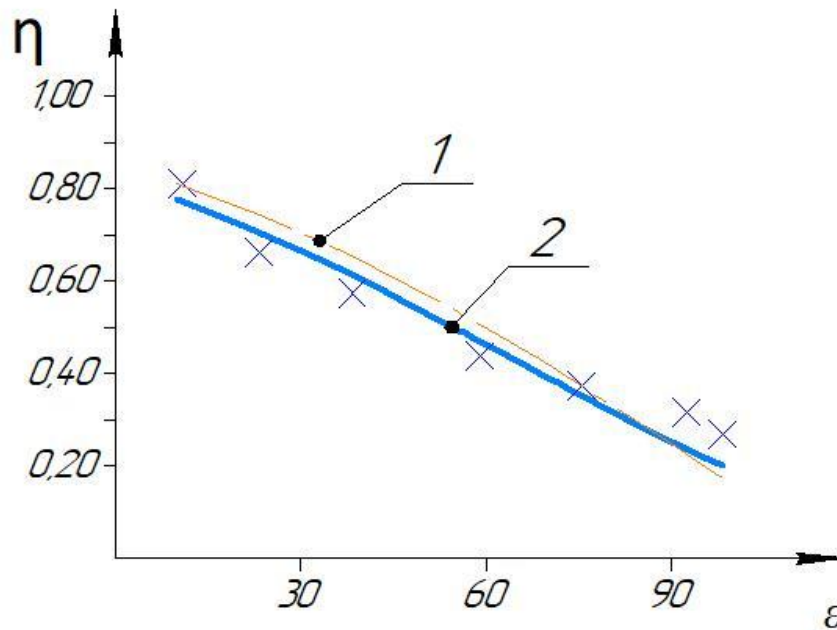


Figure10–Graph of the change in the indicator isothermal efficiency from the degree of pressure increase

Based on the experimental data, equation (10) takes the form:

$$\alpha = \lambda_g \cdot (\rho/\mu)^{0.8} W^{0.8} D^{0.2}_{equ} \quad (13)$$

Research results

Let's consider the cost of indicator work on compression when using a two-stage circuit and a single-stage circuit with a low-speed compressor. Note that, according to the well-known method, the compression polytropic coefficient for a low-speed compressor is determined according to the data of [17]. Figures 11, 12 show indicator diagrams of two-stage compression and single-stage compression using a low-speed compressor.

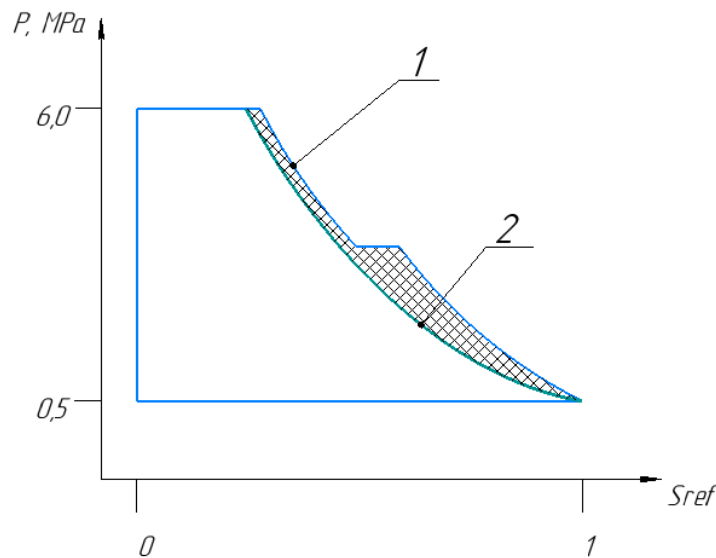


Figure 11–Indicator diagrams of two-stage compression and single-stage compression using a low-speed compressor (cycle time 2s)

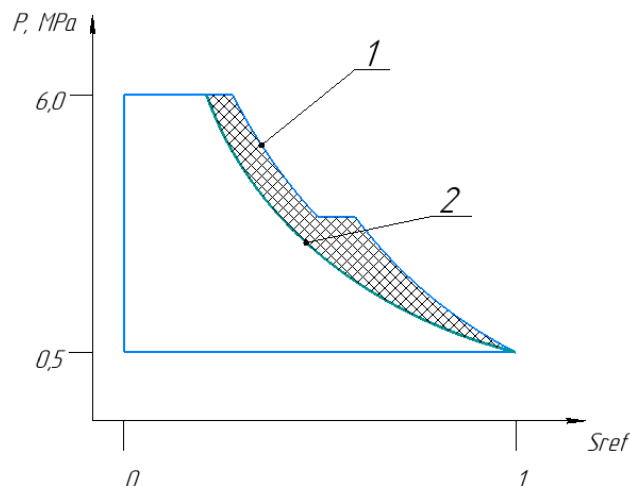


Figure 12–Indicator diagrams of two-stage compression and single-stage compression using a low-speed compressor (cycle time 4s)

The analysis of the presented graphs suggests a decrease in the indicator operation of compression when using a low-speed compressor. Line 1 corresponds to compression in a two-stage machine, line 2 corresponds to compression in a low-speed single-stage machine. In this case, the shaded area is proportional to the decrease in compression work. It can be seen that the compression line of a low-speed compressor is located to the left relative to the compression line of a two-stage compressor, that is, compression occurs in a low-speed compressor in a quasi-isothermal mode. The equivalent polytropic indicator is approximately 1.1. For a mode with a cycle time of 4 seconds, the power consumption is reduced by about 15% relative to the two-stage compression, and for a cycle time of 2 seconds – about 10%.

Thus, the exclusion of the condenser from the circuit allows, along with an increase in the efficiency of the refrigerating machine (the refrigerating coefficient increases by $10 \div 15\%$), to reduce the weight and dimensions of the refrigerating machine by 20%.

II. Conclusions

Theoretical studies have shown the possibility of replacing two-stage refrigerating machines with single-stage ones using low-speed compressors. The low rate of compression polytrope in low-speed machines makes it possible to realize compression close to isothermal. Due to this, the temperature at the end of compression is significantly lower, which allows the use of single-stage machines up to compression ratios of 100 and above. The use of such a scheme allows to increase the refrigeration coefficient by $12 \div 20\%$. At the same time, there is no need to install a condenser heat exchanger, which reduces the weight and overall dimensions of the entire installation by 20%. As can be seen from the results obtained, it is possible to obtain the liquid phase of the refrigerant in the working chamber of the compressor. For low-speed compressors, the presence of liquid is not scary and does not cause hydraulic shocks. However, the study of the condensation process of the working fluid in the compressor requires additional research and must be confirmed experimentally. The authors of this article are dealing with this issue.

Acknowledgement

This work supported by the grant from the Russian Science Foundation No. 24-29-20010.

References

- [1]. Stephen M. Hall PE. 2018. Rules of Thumb for Chemical Engineers (Sixth Edition). Chapter 23 – Refrigeration. Pages 397-411. <https://doi.org/10.1016/B978-0-12-811037-9.00023-0>
- [2]. Yuheng Du, Guohing Tian, Michael Pekris. 2022. A comprehensive review of micro-scale expanders for carbon dioxide related power and refrigeration cycles. Appl. Therm. Eng. 201 Part A. 117722. <https://doi.org/10.1016/j.applthermaleng.2021.117722>
- [3]. Amal Mtibaa, Valentina Sessa, Gilles Guerassimoff, Stephane Alajarin. Refrigerant leak detection in industrial vapor compression refrigeration systems using machine learning. Int. J. Refrig. 161, 51-61. <https://doi.org/10.1016/j.ijrefrig.2024.02.016>
- [4]. Andrey Rozhentsev. 2008. Refrigerating machine operating characteristics under various mixed refrigerant mass charges. Int. J. Refrig. 31.7. 1145-1155. <https://doi.org/10.1016/j.ijrefrig.2008.03.001>
- [5]. Maurice Stewart. 2019. Surface Production Operations. Volume IV - Pump and Compressor Systems: Mechanical Design and Specification. 655-778. <https://doi.org/10.1016/B978-0-12-809895-0.00009-0>
- [6]. Xinye Zhanq, Davide Ziviani, James E. Braun, Eckhard A. Groll. 2022. Theoretical analysis of dynamic characteristics in linear compressors. Int. J. Refrig. 109. 114-127. <https://doi.org/10.1016/j.ijrefrig.2019.09.015>

- [7]. Hyun Kim, Chul-giRoh, Jong-kwon Kim, Jong-min Shin, Yujjin Hwang, Jae-keun Lee. An experimental and numerical study on dynamic characteristic of linear compressor in refrigeration system. *Int. J. Refrig.* 32. 1536-1543. <https://doi.org/10.1016/j.ijrefrig.2009.05.002>
- [8]. S.A. Tassou, T.Q. Qureshi. 1998. Comparative performance evaluation of positive displacement compressors in variable-speed refrigeration applications. *Int. J. Refrig.* 21, 29-41. [https://doi.org/10.1016/S0140-7007\(97\)00082-0](https://doi.org/10.1016/S0140-7007(97)00082-0)
- [9]. Rajarshi Bandyopadhyay, Ole FrejAlkilde, SreedeviUpadhyayula. 2019. Applying pinch and exergy analysis for energy efficient design of diesel hydrotreating unit. *Journal of Cleaner Production.* 232. 337-349. <https://doi.org/10.1016/j.jclepro.2019.05.277>
- [10]. Xinye Zhang, Davide Ziviani, James E. Braun, Eckhard A. Groll. 2020. Experimental validation and sensitivity analysis of a dynamic simulation model for linear compressors. *Int. J. Refrig.* 117, 369-380. <https://doi.org/10.1016/j.ijrefrig.2020.04.027>
- [11]. Yocai Liang, Zhili Sun, Meirong Dong, Jidong Lu, Zhibin Yu. 2020. Investigation of a refrigeration system based on combined supercritical CO₂ power and transcritical CO₂ refrigeration cycles by waste heat recovery of engine. *Int. J. Refrig.* 118, 470-482. <https://doi.org/10.1016/j.ijrefrig.2020.04.031>
- [12]. Yusha, V.L., Busarov, S.S. & Nedovenchanyi, A.V. Experimental Evaluation of the Efficiency of Long-Stroke, Low-Speed Reciprocating Compressor Stages in Compression of Different Gases. *Chem Petrol Eng* 54, 593-597 (2018). <https://doi.org/10.1007/s10556-018-0520-1>
- [13]. S.J. James, C. James. 2010. Advances in the cold chain to improve food safety, food quality and the food supply chain. *Delivering Performance in Food Supply Chains.* Woodhead Publishing Series in Food Science, Technology and Nutrition, 366-386. <https://doi.org/10.1533/9781845697778.5.366>
- [14]. Marwam Chamoun, Romuald Rulliere, Philippe Haberschill, Jean Francois Beraill. Dynamic model of an industrial heat pump using water as refrigerant. *Int. J. Refrig.* 35, 1080-1091. <https://doi.org/10.1016/j.ijrefrig.2011.12.007>
- [15]. Marcel Ulrich Ahrens, IgnatTolstorebrov, Even Kristian Tønsberg, Armin Hafner, R.Z. Wang, Trygve MagneEikevik. Numerical investigation of an oil-free liquid-injected screw compressor with ammonia-water as refrigerant for high temperature heat pump applications. *Appl. Therm. Eng.* 219, 119425. <https://doi.org/10.1016/j.applthermaleng.2022.119425>
- [16]. Yusha, V.L., Karagusov, V.I. & Busarov, S.S. Modeling the Work Processes of Slow-Speed, Long-Stroke Piston Compressors. *Chem Petrol Eng* 51, 177-182 (2015). <https://doi.org/10.1007/s10556-015-0020-5>
- [17]. Yusha V. L., Busarov S. S. Determination of polytropic indicators of schematized working processes of air piston slow-moving long-stroke compressor stages // *Omsk Scientific Bulletin. Series Aviation-Rocket and Power Engineering.* 2020. Vol. 4, no. 1. P. 15-22. DOI: 10.25206/2588-0373-2020-4-1-15-22